Advances in Physics Theories and Applications
ISSN 2224-719X (Paper) ISSN 2225-0638 (Online)
Vol.29, 2014

Blowouts and Increase of Plasma Electrons in Beam-Driven Plasma Wakefield Accelerators

L.G. Garba[1] and Y.Y. IBRAHIM[2]
[1]*Department of Physics, Umaru Musa Yar'adua University, P.M.B. 2218 Katsina-Nigeria.*
ridwangy@umyu.edu.ng (GSM- +2348039648300)
[2]*Department of Physics, Bayero University, Kano-Nigeria.*

ABSTRACT:
The nonlinear blowout regime of the plasma Wakefield acceleration has been the subject of considerable interest due to its potential use as a next accelerator generation in high energy Physics. Much of the analytical work and simulations in this regime has been restricted to scenarios of cold background plasma in one dimension. This paper addresses the phenomenon of hot Plasma in two dimensions. We simulate beam-driven plasma Wakefield using object oriented particle-in-cell (OOPIC) code. The number density of the electron bunch was considered to be greater than the plasma density and so all of the Plasma electrons were expelled from the axis, which causes blowout of the plasma electrons. It is found that at a position where the blown out electrons return to the axis, the electron Plasma density was increased by almost 2 orders of magnitude, which further creates a strong spike in the electric field component E_z within the tail of the electron beam. These blowouts remain static throughout the simulation period.
Key Words: Beam-driven plasma wave, OOPIC and Plasma Wakefield Accelerators.

1.0 INTRODUCTION

The quest to understand the fundamental nature of matter and energy requires higher energy particle collisions, which in turn lead to larger and more expensive particle accelerators. One of the main parameters that determines the generation of high energy accelerators is the acceleration gradient[1]. The concept of plasma-based accelerators which produce extremely high accelerating gradient has become an area of growing interest since the work of Tajima and Dawson[2]. However, this Wakefield acceleration in plasmas is acknowledged as a promising method for producing beams of energetic electrons over very short distance compared to conventional accelerator technology.

Plasma-based accelerators are of great interest because of their ability to sustain extremely large acceleration gradients. The accelerating gradients in conventional radio frequency Linear accelerators (RF Linacs) are presently limited to roughly 100MV/m, partly due to breakdown which occurs on the walls of the structure. Ionized plasmas however, can sustain electron plasma waves with electric field;

$$E_0 = \frac{cm_e\omega_p}{e} \quad \text{.....(1)}$$

on the order of the non-relativistic wave breaking fields.

where

$$\omega_p = \left(\frac{4\pi n_e e^2}{m_e}\right)^{1/2} \quad \text{..... .....} \quad \text{..(2)}$$

is the plasma frequency at an electron density of n_e, c is the speed of light, m_e the electron mass and e is the charge of an electron[3&4].

1.1 Theoretical background

The most widely investigated plasma-based accelerators are the plasma Wakefield accelerator (PWFA), the plasma beat-wave accelerator (PBWA), the laser Wakefield accelerator (LWFA), including the self modulated regime and Wakefield accelerators driven by multiple electron or laser pulses[5].

Plasma-based accelerators in which the plasma wave is driven by one or more electron beams are referred to as plasma Wakefield accelerators (PWFA)[6]. The concept of using electron beam driven plasma waves to accelerate charge particles was apparently first proposed by Fainberg in 1956[7]. In such an accelerator, an electron beam (the driven beam) is sent through background plasma, consisting of electrons and positively charged ions. The plasma electrons in the vicinity of the driven beam are deflected away, while the higher-mass ions remain relatively unperturbed.

The resulting fluctuations in the plasma give rise to an electric field which has regions of alternating sign trailing behind the beam in the transverse direction. In a typical linear case, the field is a wave of wavelength λ_p (the plasma wavelength) which is inversely proportional to the square root of the plasma density. This Wakefield can then be used to accelerate and focus a second, witness electron beam for as long as it remains in the correct region of the wake.

This method of acceleration allows the energy from many electrons (in the driving beam) to be transferred to relatively few electrons in the witness beam, thus achieving very high energies over short distances. Recent experiments have created accelerating gradients on the order of 50GV/m, which are sustained over a distance of just under a meter, leading to an energy gain of 44GeV/m in some of the accelerated electrons. To enable plasma accelerators compete with large traditional accelerators, even higher accelerating gradients are necessary. To this end new experimental methods and consideration are being explored.

1.2 Plasma Wave Generation

The physical origin of the plasma wave in the PWFA is the space-charge force associated with the drive electron beam. When an electron beam propagates into the plasma, the beam density n_b generates a space-charge via Poisson's equation[5];

$$\nabla^2\varphi = e(n_e - n_i) \quad \text{.....(3)}$$

where n_e is the plasma electron density, n_i the plasma ion density and φ is the electric potential. The resulting space-charge force is given by;

$$F_{SC} = -mc^2\nabla\varphi \quad \text{..... ... ...(4)}$$

which could drive a plasma Wakefield.

The plasma electrons will respond so as to cancel the space-charge potential of the beam, i.e. the perturbed plasma density is given by;

$$\delta_n = -n_b \quad \text{..... (5)}$$

If the electron beam terminates in a short time compared to ω_p^{-1}, a plasma Wakefield of the form;

$$\delta_n = n_b \sin k_p(z - ct) \quad \text{..... ..(6)}$$

is generated. Where $k_p = \frac{\omega_p}{c}$

The axial electric field of the wake behind the beam is given by;

$$\frac{\partial E_z}{\partial z} = -4\pi e\delta_n \quad \text{..... ....(7)}$$

Therefore;

$$E_z = 4\pi e\left(\frac{n_b}{k_p}\right)\cos k_p(z - ct) \quad \text{..... (8)}$$

The peak amplitude of the wake is;

$$E_{max} = \left(\frac{n_b}{n_0}\right)E_0 \quad \text{..... ....(9)}$$

2.0 PARTICLE-IN-CELL APPROACH TO PLASMA SIMULATION

Plasma simulation with many particles started in the late 1950s, with fields obtained from Gauss' law in one dimension[8]. The next step to two and three dimension followed, but this requires a mesh for charge and current collection as well as solution of the field equations, this method was called particle-in-cell. The PIC method was codified in the 1960s-1980s by Birdsall and Longdon (1985)[9], and by Hockney and Eastwood (1988)[10]. More recent addition includes techniques for including boundaries and external circuits as well as Monte Carlo Collisions (MCC) with neutral particles.

The standard PIC–MCC scheme solves the equation representing a coupled system of charged particles and fields. The particles are followed in a continuum space while the fields are computed on a mesh. Interpolation provides the means of coupling the continuum particles and the discrete fields. A scheme for advancing the particles and fields one time step is shown in Fig.1.

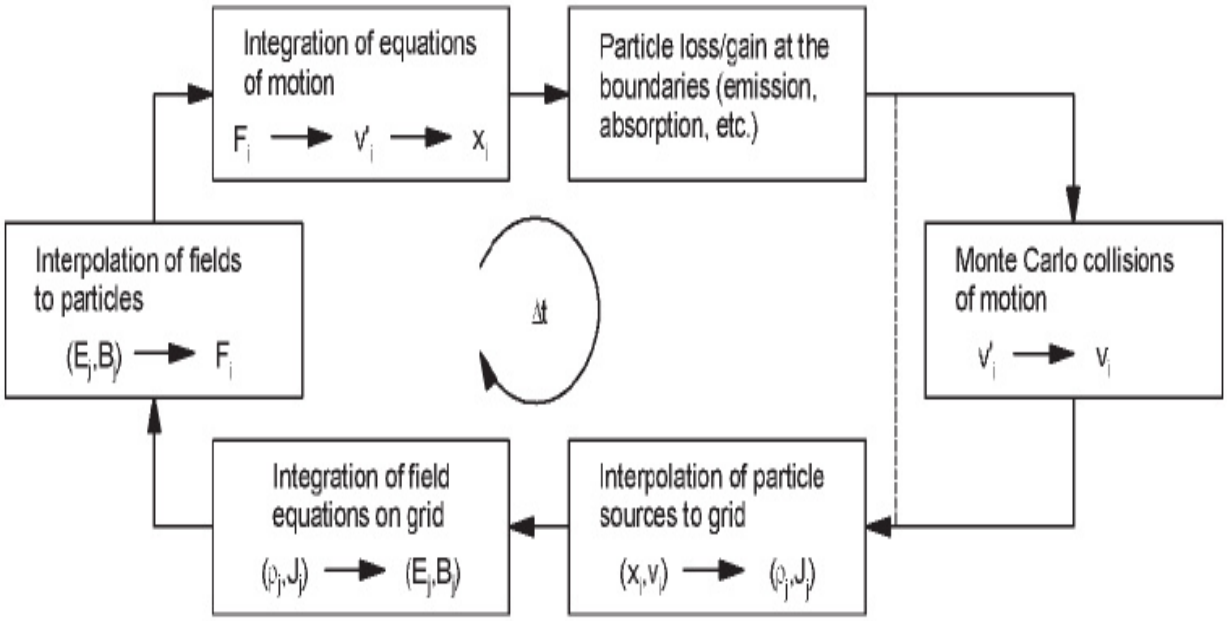

Figure.1: Flow chart for an explicit PIC-MCC scheme

2.1 The OOPIC code

The OOPIC (Object Oriented Particle-In-Cell) code was written in C++ by Verbancoeur (1995)[11] at the University of California, Berkeley and the Tech-X Corporation[12]. The code started as a pioneering effort to apply object oriented techniques to plasma simulation codes.

OOPIC is widely used by the plasma and beam-microwave communication worldwide, with application ranging from high pressure discharges to relativistic microwave devices.

The code models two spatial dimension in both Cartesian (x,y) and cylindrical (r,z) geometry, including all three velocity components with both electrostatic and electromagnetic models available. All three components of both the electric and the magnetic fields are modeled but there is no spatial variation along the ignored coordinate.

The code presently supports a nonuniform orthogonal mesh and arbitrary placement of most boundary condition on that mesh. Static magnetic fields can be added analytically using the equation evaluator, or read from internal file. A number of different charge and current weighting algorithms are available as well as Poisson and Longdon-Marder divergence corrections for non-conservative current weighting scheme. The code includes a fully relativistic model for inertial particles as well as on a Boltzmann model for inertia less electrons. Particles and fields can each run independently sub cycled time steps, improving computational efficiency. A temporal filtering scheme reduces high frequency noise and a material digital filtering algorithm reduces short wavelength noise.

2.2 PWFA Simulation

In this section, OOPIC simulations of plasma afterburner concept is presented, which is a scaled up version of E-157 PWFA experiment at SLAC. The E-157 operates in the 'blowout' regime of the PWFA meaning the number density of the electron bunch is greater than the plasma density, so that all of the plasma electrons are expelled from the axis in the vicinity of the electron bunch. The EPW generated by the electron bunch is expected to accelerate electrons in the tail of the bunch to higher energies.

2.2.1 Physical constants used throughout the input file:

These are the constants built in and do not need to be defined in OOPIC pro input file. Some of these constants used in this simulation are listed below:

Table 1: Physical operators

S/N	OPERATOR	VALUE
1	Pi	3.14159
2	C	2.998e08
3	Electron Mass	9.1095e-31
4	Unit Mass	1.6606e-27
5	Lithium Mass num.	6.949

The following high-energy electron beam parameters are also used.

Beam energy = $50x10^{9}$eV

Total number of beam = $2x10^{10}$

Root mean square beam – Radius = $1x10^{-5}$m

Root mean square beam length = $4x10^{-5}$m

2.2.2 The Grid:

This is used to specify the size, shape, geometry and other characteristics of the numerical grid superimposed upon the simulated system. It establishes a correspondence between the numerical grid and geometrical parameters of the system. The table below gives details of the grids used in this simulation

Table 2: Grid values

S/N	*PARAMETER*	*VALUE*	*DESCRIPTION*
1	Geometry	0	Cylindrical geometry (r,z)
2	J	384	Number of cells in z direction
3	K	64	Number of cells in r direction
4	X1S	0.0	Lower coordinate in z direction
5	X1F	$2x10^{-5}$	Upper coordinate in z direction
6	X2S	0.0	Lower coordinate in r direction
7	X2F	$3x10^{-5}$	Upper coordinate in r direction
8	N_1	1.0	Scaling parameter for nonuniform gird in z direct.
9	N_2	1.0	Scaling parameter for nonuniform grid in r direct.

2.2.2 Control

The control element is to specify the time step for the simulation, initial static E & B fields' parameter. For example the time step used in this simulation was $dt = 0.43 \times \frac{rGridsize}{speed\ of\ light} = 6.73 \times 10^{-16}s$

A moving window was enabled, which will enable it move fields and particles in the simulation one cell to the left at the speed of light with each time step. However, boundaries are not moved. Additionally a load with the name "shift load" will be loaded whenever a shift occurs

2.2.3 The beam parameters

The following were some of the beam parameters used in the simulation.

Table 3: Beam parameters

S/N	PARAMETER	VALUE
1	Number of cells	512
2	Number of beams per cell	1000
3	Total number of beam particles	512000
4	Beam number ratio	$3.9x10^{4}$
5	Beam density	$2x10^{23}cm^{-3}$

Table 4: Plasma parameters

S/N	PARAMETER	VALUE USED
1	Plasma density	$2x10^{22}cm^{-3}$
2	Number of plasma part. Per cell	10
3	Simulation volume	$678.58x10^{-15}m^3$
4	Total number of plasma	$13.572x10^9$
5	Number of plasma part.	245760
6	Plasma number ratio	$5.523x10^4$
7	Gas temperature	0.088eV
8	Plasma temperature	O(cold)

2.2.5 MCC (Monte Carlo Collisions)

This element specifies the Monte Carlo collisions parameters used to model collisions of the particles with the background gases which resulted in the ionization of the background gases and the production of a pre-defined species of particles.

However, the gas used in this simulation was lithium gas, with the following properties:

Gas temperature = 0.088ev

Gas density = $2x10^{23}cm^{-3}$

Gas pressure = $1.2x10^{-21}$ gas density x gas temperature

= $1.2x10^{-21}x2x10^{23}x0.088$

= 0.2112×10^2 torr

2.2.6 Boundary conditions

The definition of a number of physical boundary configurations that can be encountered is specified

The boundary conditions are:

i) The simulation region must be bounded by either conductors or insulators, in order to capture lost particles

ii) Conductors were chosen, to avoid any charge build up

iii) The choice of conducting boundary conditions means that electric fields parallel to the boundaries are forced to zero, however, fields near the boundaries of the simulation must be small anyway to accurately model semi-infinite plasma.

3 RESULTS AND DISCUSSION

Fig.2 shows the initial 30 GeV beam in cylindrical coordinates. The particles are variably weighted with radius, allowing for a particle density that is independent of radius, while the initial charge density is Gaussian in both the longitudinal and transverse directions. The beam enters the simulation region from the left with zero energy spread and zero emittance, propagating to the right with a velocity very close to the speed of light. Once the beam is close to the right edge of the simulation region, the moving window algorithm is invoked; keeping the beam in the same relative location. The plasma ions are modeled as a stationary uniform background, while the plasma electrons are modeled with uniformly distributed particles with initially zero velocity. Because the peak beam density $n_b = 2 \times 10^{23} cm^{-3}$ exceeds the plasma density $n_e = 2 \times 10^{22} cm^{-3}$, the plasma is said to be under dense and the self fields of the beam cause "blowout" of the plasma electrons (Fig. 3), which is the origin of the strong plasma wake.

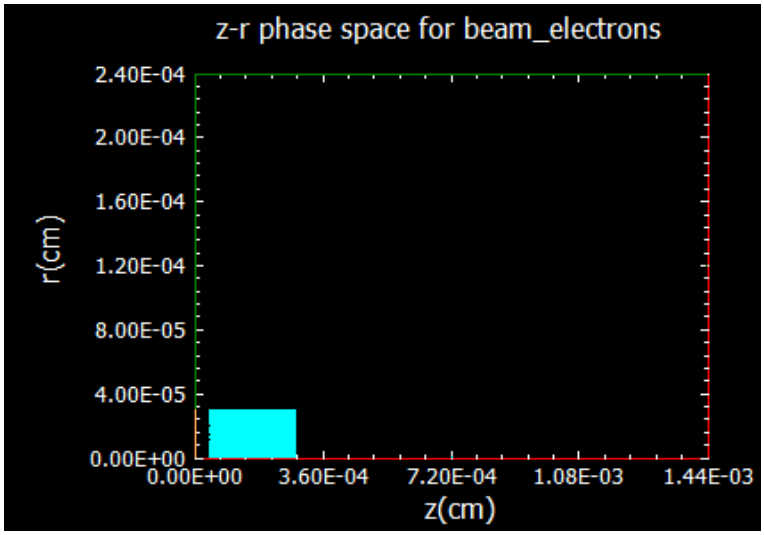

Figure 2: The z-r phase space for beam electrons.

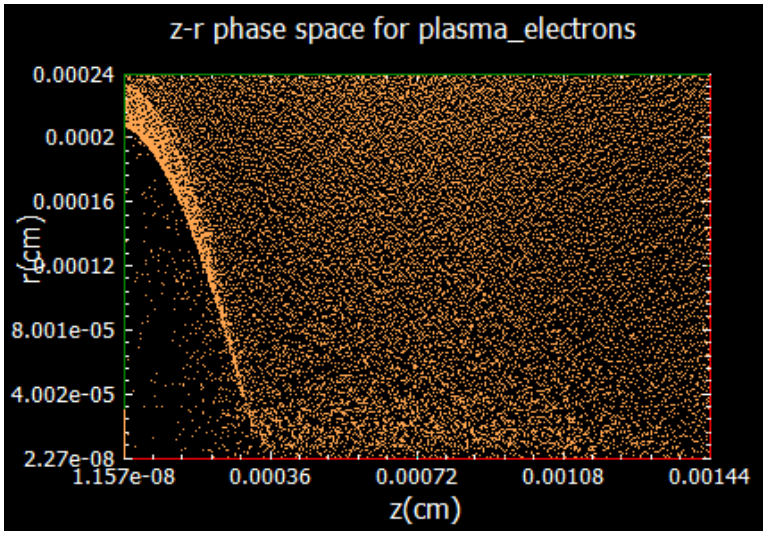

Figure 3: The z-r phase space for plasma electrons showing blowout of electrons from the axis at t = 1.113×10^{-12}s

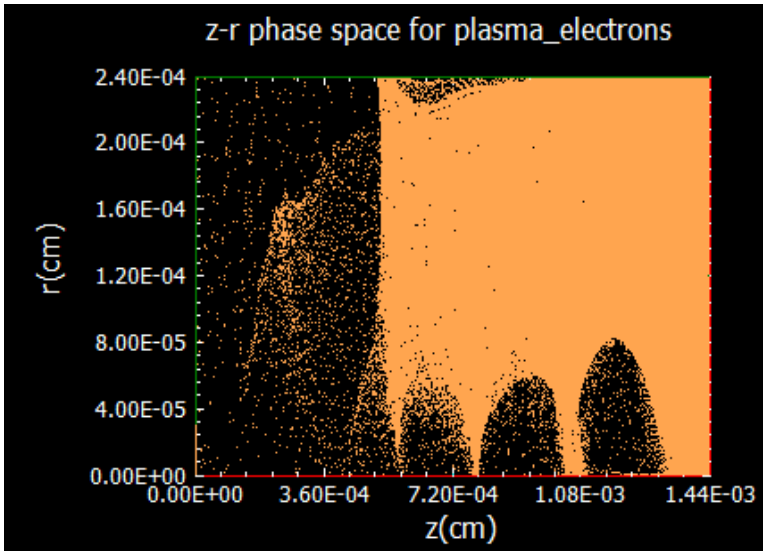

Figure 4: The z-r phase space for plasma electrons showing the Wake in the plasma electron distribution for t = 7.72×10^{-12}s

Fig.4 shows the plasma electrons after the 30GeV electron beam has propagated for t=7.72x10^{-12}s. This "wake" in the particle distribution is what drives the EPW (Fig.6). Plasma electrons near the head of the electron beam are driven away from the axis. Most of these blown out plasma electrons return to the axis near the tail of the electron beam. In the vicinity of the small region centered on z = 1.08x10^{-3}, r = 0 (fig.5), where the blown out electrons return to the axis, the electron plasma density is increased by almost 2 orders of magnitude. This localized increase in the charge density creates a strong spike in the electric field component *E*z within the tail of the electron beam (Fig.7(a) and (b)). Also, the space charge of the unneutralized plasma ions in the wake generates a strong radial electric field component, which focuses the bulk of the electron beam. The structure of the plasma wake is independent of the beam radius and remains approximately static throughout the simulation.

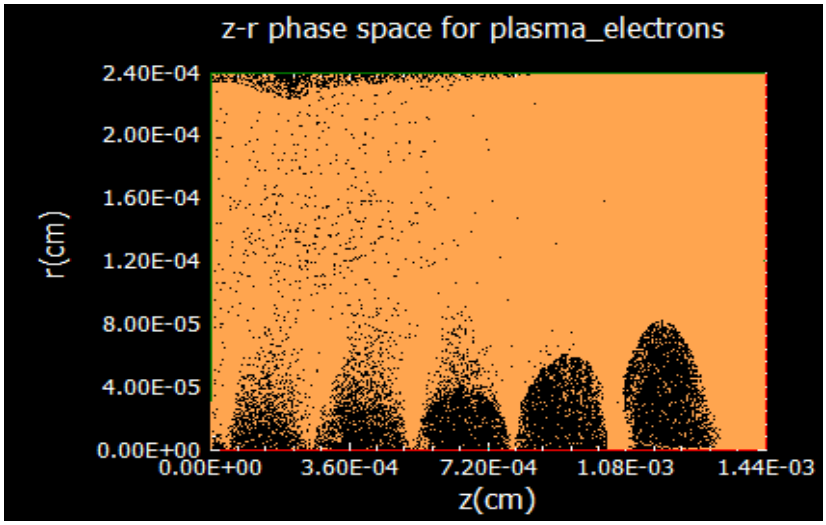

Figure 5: The z-r phase space for plasma electrons showing blowout of electrons from the axis and formation of a large plasma wake. The plasma wake is approximately static throughout the simulation.

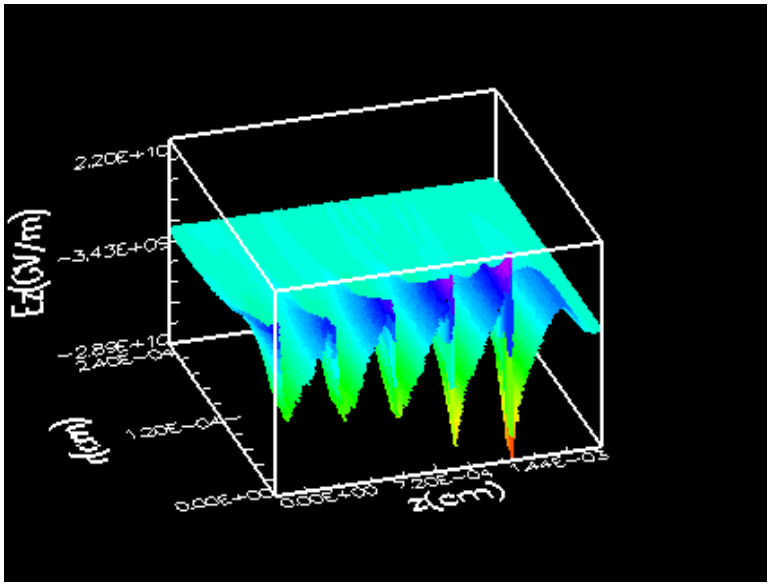

Figure 6: Electric field of the electron pulse

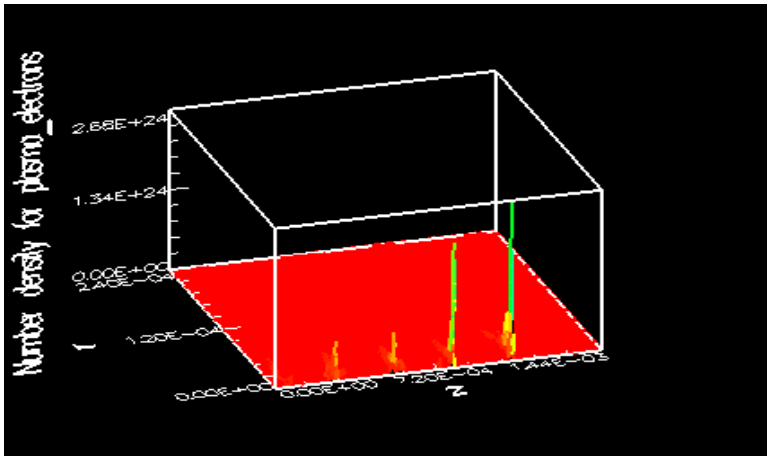

Figure 7(a): Plasma electrons density spikes at the tails of the electron pulse

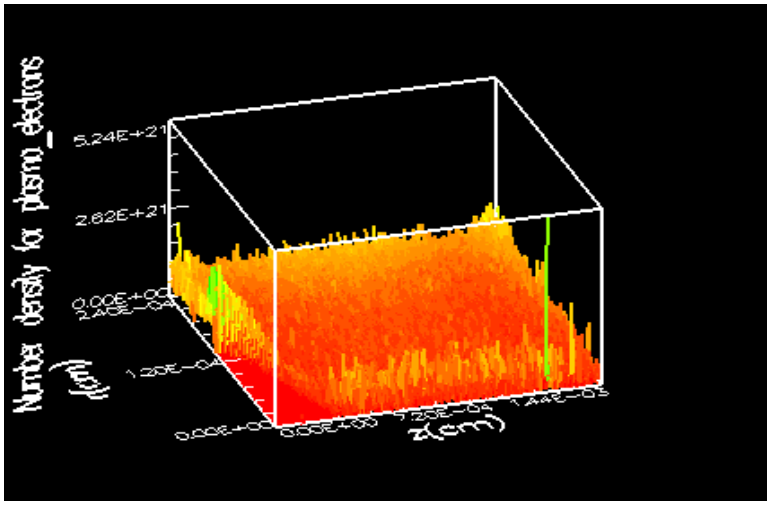

Figure 7(b): Plasma electrons density spikes at the tails of the electron pulse.

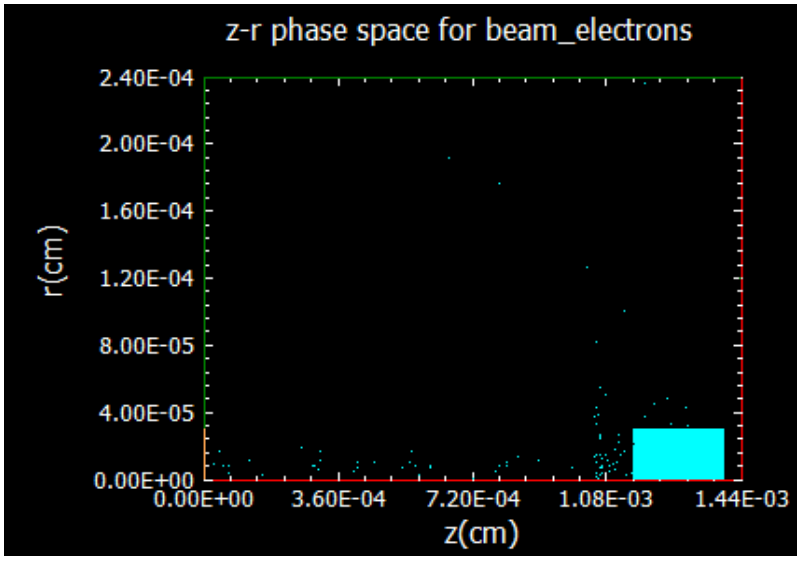

Figure 8: The z-r phase space for beam electrons at t = 1.099×10^{-11}s

Fig.8: shows the 30 GeV electron beam after t = 1.099×10^{-11}s of propagation, corresponding to two betatron wavelengths. The head of the beam remains largely unaffected because it does not see the wake.

However, Fig.6 shows the longitudinal electric field *Ez* generated by the wake, in GV/m, after 80 cm of propagation. The large peak value of approximately -3.43GV/m coincides with the peak in the plasma electron density at the point where plasma electrons in the wake return to the axis of symmetry. With higher resolution,

the peak field value on axis is enhanced (greater than 1 GV/m), but very little difference is observed in the structure of the field away from the peak. Thus, the present resolution is adequate to model acceleration of electrons within the tail of the 30 GeV beam. The features seen in Fig. 6 are approximately static during the full 100 cm of beam propagation.

4 SUMMARY AND CONCLUSION

It can be seen in Fig.6 that *Ez* is positive for large values of z, which decelerates the electrons in the center of the 30 GeV beam distribution. This energy taken from the beam provides the energy needed to drive the wake. For small values of z, *Ez* is large and negative, which accelerates electrons in the lower density tail of the electron beam distribution. The goal of the E-157 experiment is to measure the energy increase of the tail particles and thus confirm the existence of the strong accelerating electric fields.

REFERENCES

[1] Ruth, R.D., Chao, A.W., Morton, P.L. and Wilson, P.B. (1984). A Plasma Wakefield accelerator. *Stanford Linear Accelerator Centre, SLAC-PUB*-3374.

[2] Wurtele, J.S. (1993). The role of plasma in advanced accelerators. *Physics Fluids B.***5** (7):2363-2370.

[3] Dawson, J.M. (1959). Nonlinear electron oscillations in cold plasma. *Physical Review.***133**:383 387.

[4] Akheizeir, A.I. and Polovin, R.V. (1956). Theory of wave motion of electron plasma. *Zh. Eksp. Teor. Fiz*. **30**:915-928.

[5] Esarey, E. and Sprangle, P. (1996). Overview of plasma based accelerator concepts. *IEEE Transactions on plasma science.***24** (2):252:288.

[6] Berezin, A.K., Fainberg, Y.B., Kiselev, V.A., Linnik, A.F., Uskov, V.V., Balakirev, V.A., Onishechendo, I.N., Sidelnikov, G.L. and Sotnikov, G.V. (1994), Wake field excitation in plasma by a relativistic electron pulse with a controlled number of short bunches. *Fizika plazmy.***20**:663-670.

[7] Fainberg, Y.B., Balakirev, V.A., Onishehendo, I.N., Sidelnikov, G.L. and Sotnikov, G.V. (1994) Wakefield excitation in plasma by a train of relativistic electron bunches. *Fizika Plazmy.***20**:674-681.

[8] Bruhwiler, D.L., Giacone, R.E., Cray, J.R., Verboncoeur, J.P., Mardahl, P. and Essarey, E.(2001). Particle-in-cell simulations of plasma accelerators and electron neutral collisions. *Physical Review special topics.* **4**(101302):1-13.

[9] Birdsall, C.K. and Langdon, A.B. (1985). Plasma physics via computer simulation. *McGraw Hill, New York*.

[10] Hockney, R.W. and Eastwood, J.W. (1988). Computer simulation using particles. *IOP. Bristol, UK,* 1988.

[11] Verboncoeur, J.P., Langdon, A.B. and Gladd, N.T. (1995). An Object-Oriented electromagnetic PIC code. *Computer Physics Communication.* **87**:199-211

[12] Giacone, R.A., Govil, R. and Wheeler, S.J. (2000).In proceedings of the 7th European particle accelerator conference, Vienna, 2000. http://accelconf.web.cern.ch/Accelconf/e00/index.html. 907.\